Synthesis, characterization and spectral studies of novel Eu^{3+} based phosphors and its solid solutions

A Report Submitted for fulfillment for Master of Science in Chemistry

Submitted by

Nikhil Bansal

Roll No- 413CY2003

Under the guidance of

Dr. V. SIVAKUMAR

DEPARTMENT OF CHEMISTRY

NATIONAL INSTITUTE OF TECHNOLOGY,

ROURKELA-769008, ODISHA

MAY-2015

Department of Chemistry

National Institute of technology,

Rourkela, Odisha, India-769008

<u>Certificate</u>

This is to certify that the thesis entitled "**Synthesis, characterization and spectral studies of novel Eu^{3+} based phosphors and its solid solutions**" submitted by **Mr. Nikhil Bansal** to the National Institute of Technology, Rourkela for the award of degree of Master of Science is a bonafide record of research work carried out by him under my supervision. The contents of this thesis, in full or in parts, have not been submitted to any other Institute or university for the award of any degree or diploma.

Rourkela-769008   Research Guide

Date: 05/05/2015

Dr. V. SIVAKUMAR

DECLARATION

I **Nikhil Bansal** hereby declare that this project report entitled "**Synthesis, characterization and spectral studies of novel Eu^{3+} based phosphors and its solid solutions**" is the original work carried out by under the supervision of **Dr. V. Sivakumar**, Department of Chemistry, National Institute of Technology, Rourkela, Odisha and the present work or any other part thereof has not been presented to any other University and Institution for the award of any other degree regarding to my belief.

(Nikhil bansal)

ACKNOWLEDGEMENT

Table of Contents

Abstract

Tungstate and molybdate based metal oxides with substituted Eu^{3+} based phosphors are promising red emitting phosphor materials for white LEDs. In the present research, a series of novel red phosphors including La_2GdBWO_9 as a host and doped $La_2Gd_{0.9}Eu_{0.1}BW_{1-x}Mo_xO_9$ (x = 0 − 0.4, insteps of 0.1) samples were prepared by the conventional solid state reaction. The phase formation and transformation of the synthesized compositions was investigated by powder X-ray diffraction, DRS studies and photoluminescence properties were studied as a function of the Mo/W ratio. All the compositions show broad charge transfer (CT) band due to CT from O to W/Mo and red emission due to Eu^{3+} ions. Eu^{3+} substituted compositions show high red emission intensity under NUV/blue ray excitation as well as the emission of the phosphor shows very good CIE (Commission Internationale de l'Eclairage) chromaticity coordinates ($x = 0.6647$, $y = 0.3349$). Band gap of $La_2Gd_{0.9}Eu_{0.1}BW_{1-x}Mo_xO_9$ (x = 0 − 0.3, insteps of 0.1) becomes narrower than that of host La_2GdBWO_9 by introducing Mo^{6+}. The obtained results are reveals that the investigated phosphors are potential phosphors for LEDs.

Chapter 1

1. Introduction to Luminescent Materials

1.1 Luminescence

A luminescent material (also called phosphors) is a solid which transforms certain forms of energy into electromagnetic radiation over and above thermal radiation. When the solid is exposed to heat (temperature $> 600°C$) it emits infrared radiation, this is called thermal radiation not luminescence. In general, the luminescent materials emits in the visible region, however certain cases in also emits in the other regions, such as ultraviolet or infrared. Luminescence materials can be excited by many forms of energy. Photoluminescence is excited by electromagnetic radiation, cathadoluminescence by beam energetic electrons, electroluminescence by an electric voltage, X-ray luminescence by X rays, chemiluminescence by the energy of a chemical reaction, and so on. The various process occurring in the luminescent materials is shown in Fig.1. The system contains a host lattice and a luminescent center, often called an activator. For example, Al_2O_3: Cr^{3+} and Y_2O_3: Eu^{3+}.in which the host lattices are Al_2O_3 and Y_2O_3, the activators are Cr^{3+} and Eu^{3+} ions.[1]

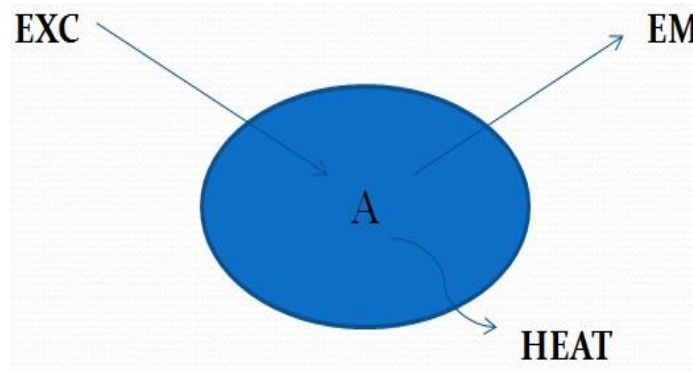**Fig1.** A luminescent ion A in its host lattice.EXC: excitation; EM: emission

1.2 Excitation and Emission

The luminescence processes in some inorganic systems is shown in Fig. 2. The exciting radiation is absorbed by the activator, raising it to an excited state. The excited state photon comes back to the ground state by emitting the photons. This suggests that this process can occur

in every system; however in reality it is not true. There are some system where the radiative process is efficient whereas the other systems wherein the non-radiative process dominant. During this process the energy in the excited state is used to for the lattice vibrations (to heat the host lattice). In order to make efficient luminescent materials it is necessary to diminish this non-radiative process.
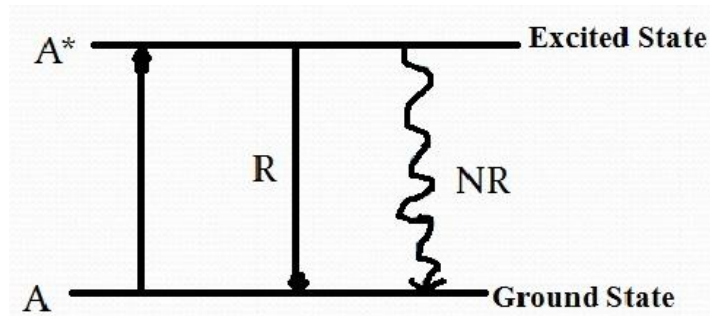

Fig2. Schematic energy level scheme of the luminescent ion A. the asterisk indicates the excited state, R the readiative return and NR the nonradiative return to the ground state.

A well known example, viz. the lamp phosphor $Ca_5(PO_4)_3F$: Sb^{3+}, Mn^{2+}. UV radiation is not absorbed by Mn^{2+} (due to forbidden transition) and hence the sensitizer Sb^{3+} been used to absorb the incident photons (UV radiation from the Hg). Under UV excitation the phosphor emits white which are due to blue emitting Sb^{3+} and yellow emitting Mn^{2+}. Since the Mn^{2+} ion was not excited directly, the excitation energy was transferred from Sb^{3+} to Mn^{2+}(see Fig3.) in which Sb^{3+} acts as sensitizer and Mn^{2+} acts as activator. The concentrations of the luminescent centers are of the order of a 1 mol %, and that the centers are scattered at random over the host lattice.[2]

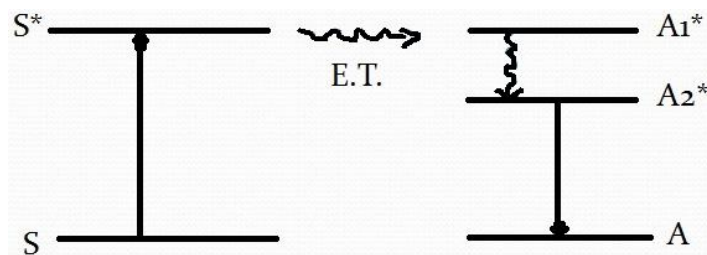**Fig3.** Energy transfer from S to A. The S to S* transition is the absorption (or excitation), the A_2* to A transition the emission. The level A_1*, populated by energy transfer (E.T.), decays non-radiatively to the slightly lower A_2* level.

The energy difference between the excitation band and emission band is called "Stokes shift"". The larger the shifting of excited state and ground state, the larger will be the stokes shift and broader the optical bands.
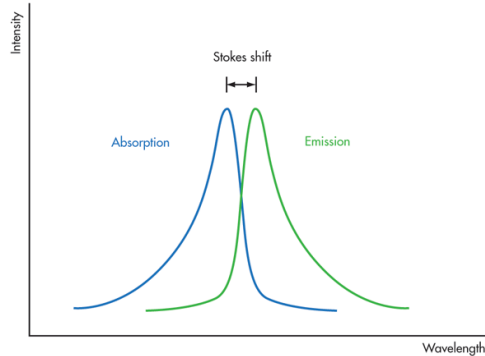

Fig4. Figure of Stokes shift

1.4 The Influence of the Host Lattice

There are some major factors which are responsible for various spectral properties of a given ion in different host lattices such as: *Covalency:* For increasing covalency in the host lattice, the interaction [5-8] between the electrons is reduced, since they spread out over wider orbitals. Consequently, electronic transitions between the energy levels with an energy difference which is determined by electron interaction shift to lower energy for increasing covalency. This is known as nephelauxetic (electron cloud expanding) effect. Higher covalency means also that the electro-negativity difference between the constituting ions becomes less, so that charge-transfer (CT) transitions between these ions move to lower energy. For example the CT absorption band of Eu^{3+} in the YF_3 was observed to be at higher energy with the comparison of more covalent oxide Y_2O_3. *Crystal field:* This is the electric field at the site of the ion under consideration due to the surroundings. The spectral position of certain optical transitions is determined by the strength of the crystal field, the transition metal ions are the most well-known and clear example. In addition the crystal field is responsible for the splitting of certain optical transitions. In general, different host lattices → different crystal fields → different splitting.

In other words the optical center can serve as a probe of the surroundings: observed splittings yield the symmetry of the site. Point defects in the crystal structure yield also a contribution to the broadening of bands.

1.4 Rare Earth Ions (4f^n)

The rare earth ions are characterized by an incompletely filled 4f shell. The 4f orbital lies deeply inside the ion and is shielded from the outer environment by the filled 5s^2 and 5p^6 orbitals. Therefore the influence of the host lattice on the optical transitions within the 4f^n configuration is small. The diagram represents the energy levels for trivalent lanthanide ions. This diagram is useful because the energies of the J multiplets vary by only a small amount in different host crystals. The diagram allows rapid recognition of the energy levels in new hosts, and has been an essential tool in the design of materials suitable for phosphors or lasers. Relaxation of the parity selection rule is due to lattice vibrations but that have very weak influence [3]. More valuable are the uneven components of the crystal field which are present when the rare earth ion occupies a crystallographic site with no inversion symmetry. These uneven mix a small amount of opposite-parity wave functions (like 5d) into the 4f wave functions. In this way the intra-configurational 4f^n transitions obtain at least some intensity. Spectroscopists say it in this way: the (forbidden) 4f→4f transitions extract some intensity from (allowed) 4f→5d transition [4, 5, 6].
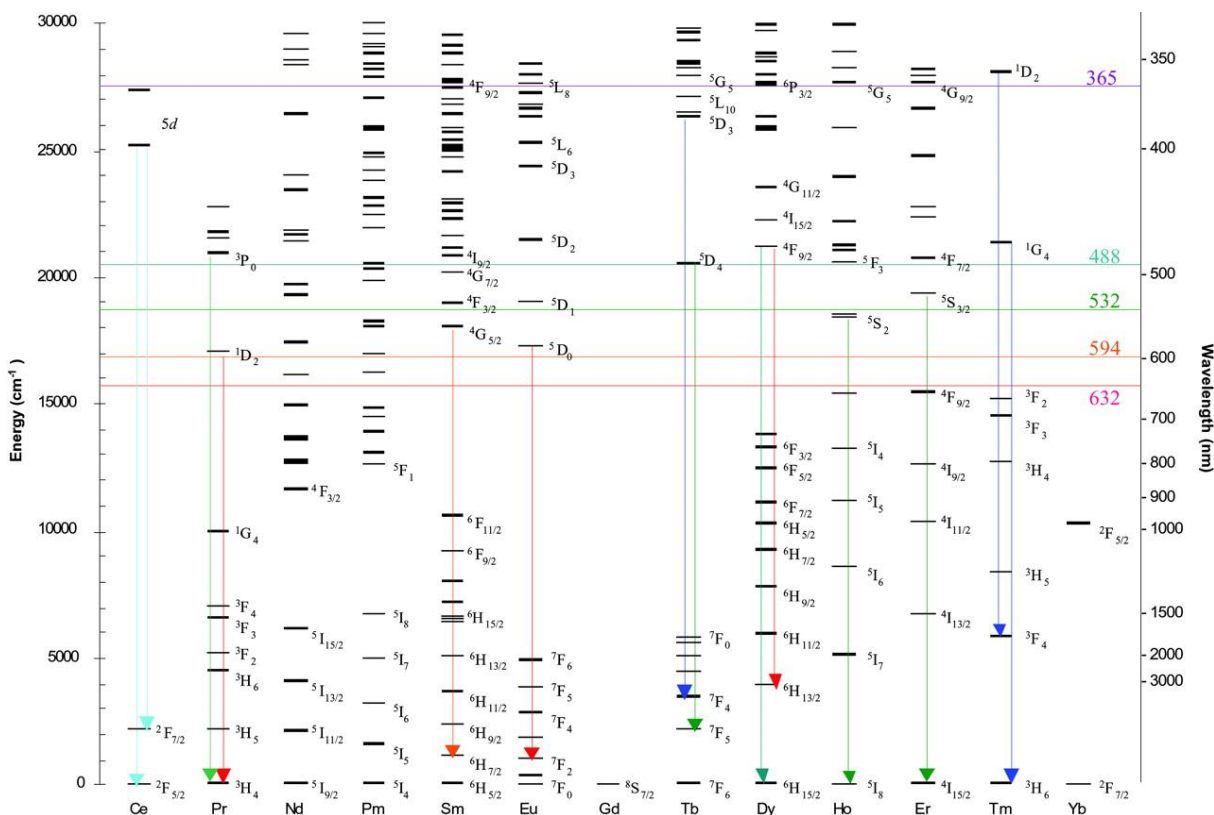

Fig 5. Dieke diagram for rare earth ions (source: wikipedia)

1.5 The Rare Earth (RE) ions (4f-5d and Charge- Transfer (CT) Transitions)

The allowed optical transitions of the rare earth ions are of two types: 1. Charge transfer transitions ($4f^n \rightarrow 4f^{n+1}L^{-1}$, where L-ligand) 2. $4f^n \rightarrow 4f^{n-1}5d$ transitions.

The transitions are allowed and give broad spectral bands in the UV to visible regions. The trivalent RE ions have a tendency to convert itself into divalent state (Sm^{3+}, Eu^{3+}, Yb^{3+}) and show CT absorption bands in the ultraviolet (UV) region. The trivalent RE ions that have a tendency to become tetravalent (Ce^{3+}, Pr^{3+}, Tb^{3+}) show 4f $\rightarrow$ 5d absorption bands in the UV region [7].

1.6 Rare Earth Ions (Line Emission)

The 4f electrons are well shielded from the outer environment. The energy levels are in reality split by the crystal field. As this splitting is very little with the comparison of transition elements due to shielding of s and p orbital, rare earth ions have less intense splitted peaks.

Gd^{3+} ($4f^7$)

Gd^{3+} ion has a half filled 4f shell which gives a very stable $^8S_{7/2}$ ground state. As an outcome the emission of Gd^{3+} is in the ultraviolet region. The $^8S_{7/2}$ level (orbitally nondegenrate) cannot be split by the crystal field. This limits the low temperature emission spectrum to one line, viz. from the crystal field level of the $^8P_{7/2} \rightarrow ^8S_{7/2}$. [8]

Eu^{3+} ($4f^6$)

The emission consists usually of lines in the orange- red region. The red emission is found a vital application in lighting and display technologies. These lines are correspond to transitions from the excited $^5D_0$ level to the ^7D_J (J=0, 1, 2, 3, 4, 5, 6) levels of the $4f^6$ configuration. Since the $^5D_0$ level will not be split by the crystal field (because J=0), the splitting of the emission transitions yields the crystal-field splitting of the ^7F_J levels. In addition to these emission lines, one observes often also emission from higher ^5D levels, viz. $^5D_1$, $^5D_2$ and even $^5D_3$. The $^5D_0 \rightarrow ^7F_J$ emission is very appropriate to study the transition probabilities of the sharp spectra features of the rare earths. If a rare earth ion occupies in the crystal lattice site with inversion symmetry, optical transitions between levels of the $4f^n$ configuration are strictly forbidden as electric-dipole

transition (parity selection rule). They can only occur as (the much weaker) magnetic-dipole transitions which obey the selection rule $\Delta J = 0, \pm 1$ (but $J=0$ to $J=0$ forbidden) or as vibronic electric-dipole transitions. If there is no inversion symmetry at the site of the rare earth ion, the uneven crystal field components can mix opposite-parity states into the $4f^n$-configurational levels. The electric-dipole transitions are now partially allowed and appear as (weak) lines in the spectra, the so- called forced electric-dipole transitions. [5, 9].

A clear example is the charge-transfer excitation of the Eu^{3+} luminescence, a process which is of large importance for applications. Consider the red phosphors with composition Y_2O_3: Eu. Excitation at 254 nm in the charge-transfer state is followed by efficient red emission ($^5D_0 \rightarrow ^7F_2$) within the $4f^6$ configuration was observed. If the charge-transfer state shifts to lower energy by host modification, the efficiency of the luminescence upon charge-transfer excitation decreases. This is due to an increasing probability of the non-radiative transition from the charge-transfer state to the $4f^7$ levels. [10]

1.7 Phosphor

In order to get the desired wavelength (color), phosphors are synthesized doping with transitional ions like Mn, Bi and rare earths like Eu, Tb, Ce etc. The phosphors materials that are used in the fluorescent lamp are primarily convert the UV emission of the rare gas/ mercury discharge plasma into white light. There are so many phosphor materials that are discovered but many of the potential phosphor candidates are ruled out due to their direct contact with mercury discharge. For example, sulphide based phosphors (ZnS) cannot be used, since they react with Hg. Therefore, oxides based phosphors are used as the hosts for these applications. In earlier, calcium halophosphate based phosphors are used in lamps. As much as the progress in the field of phosphor is concerned, Eu^{2+} ion was frequently used as an activator ion in various host lattices. Due to the shielding effect of the outer shells, the 5d electrons split easily by the crystal field around it. Thus the peak position of Eu^{2+} emission strongly depends on the Eu^{2+} ions surrounding, consequently, Eu^{2+} ions can emit from near UV to red region of the spectrum. In addition, Eu^{3+} is also used as an activator due to unique feature in the spectral lines in the visible region (orange or red).

1.7.1. Lanthanide based phosphors:

The color which is produced from halo phosphate lamp phosphor is not ideal or suitable and it is necessary to produce higher CRI (Color Rendering index). The first report of a fluorescent lamp based on new concept was made by Haft and Thornton in 1972. The phosphor combination of $Sr_3(PO_4SrCl:Eu^{2+})$, $Zn_2SiO_4:Mn^{2+}$ and $Y_2O_3:Eu^{2+}$ (blue, green, and red) with color temperature 4200K. However, this concept not been commercialized due to the poor maintenance characteristics of the phosphors [1].

1.7.2. Blue emitting phosphors:

The commercially used blue emitting phosphors in tricolor fluorescent lamps are $BaMgAl_{10}O_{17}$ and $(Sr, Ba,Ca)_5(PO_4)Cl:Eu^{2+}$. The synthesis is generally accomplished under a reduced atmosphere (reduction of Eu^{3+} to Eu^{2+}). The blue phosphors represent only a minor weight fraction of the tri-phosphor. However, blends with higher amount of the blue emitting components are necessary for higher color temperature (6500 K).
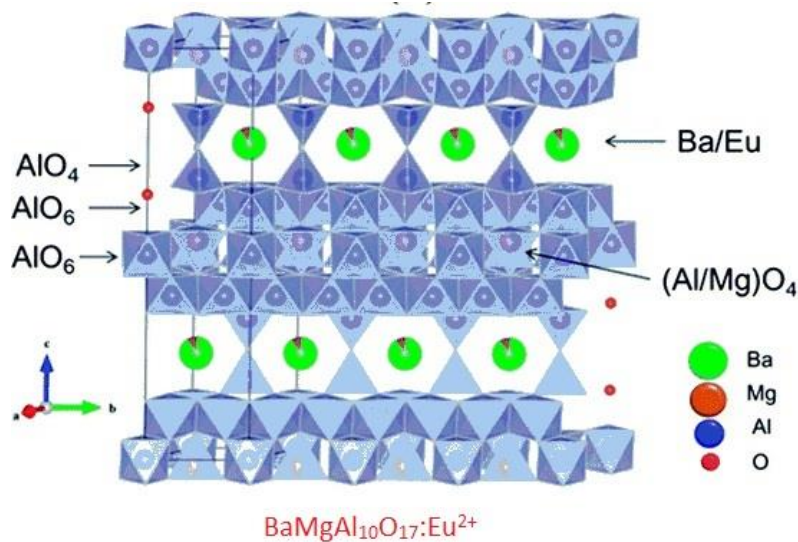

$BaMgAl_{10}O_{17}:Eu^{2+}$

Fig 6. Crystal structure of BAM (drawn by using ball and stick model)

1.7.3. Green emitting phosphor (Ex: LaPO4: Ce, Tb)

This phosphor is rapidly gained popularity as an alternative to the CMA: Tb^{3+} phosphor due to ease of manufacturing ($\sim 1000^{\circ}$ C) and lower the concentration of Tb is good enough for optimum performance.
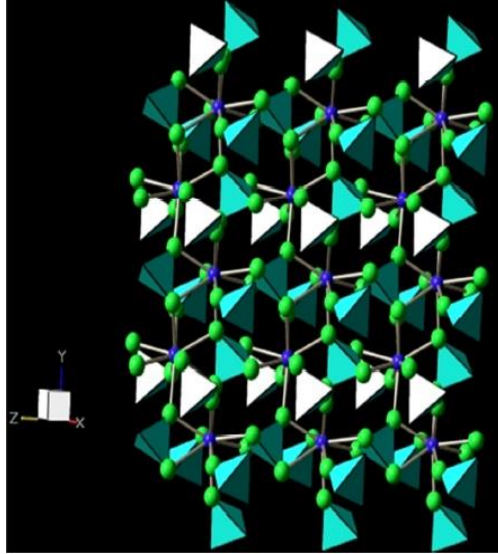
Fig7. Crystal structure of $LaPO_4$ [along (100)]

1.7.4. Red emitting phosphor: Ex: $Y_2O_3:Eu^{3+}$

$Y_2O_3:Eu^{3+}$ phosphor fulfills all the requirements for a good red emitting phosphor. By using different compositions of the Eu and Y, one may end up with good efficient phosphor with appropriate color purity. But the high cost of Eu based phosphors prohibits such compositions for practical applications. Research aimed at replacing this phosphor emission with less expensive alternatives.
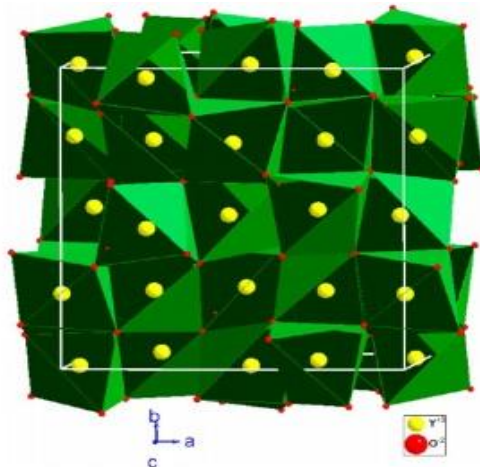

Fig8. Structure of $Y_2O_3:Eu^{3+}$

1.7.5. Rare earth based phosphors:

The alkali earth aluminates containing rare earth ions are functional inorganic materials that are used for the synthesis of blue and red emitting phosphors [11-13]. These phosphor materials are generally used for such devices "glow-in-dark" objects as, direction indicators, safe helmets and signs, varieties of toys, robber shoe soles and the like due to their better safe, excellent photo resistance, chemical stability, very bright and long lasting afterglow with no radio-active radiations and hence forms the important materials in various ceramics industries [14].

In recent years, $SrAl_2O_4$ and $Sr_4Al_{14}O_{25}$ phosphors doped with Eu^{2+} and Dy^{3+} ions have been regarded as excellent phosphors and attracted the scientist's interest [15-16]. For the development of phosphorescent properties, research has been focused on concerning extracts, different compositions, various molar ratio and the planning methods [14-15]. Wu *et al.* reported that the control of particle size by using the sol-gel and co-precipitation methods [16]. It was found that the shape and size of phosphor particles plays a vital role for the fluorescence properties of $Sr_4Al_{14}O_{25}:Eu^{2+}$ phosphor. When the particle size reaches the nano-scale, new properties are appeared like the blue shift of emission intensity [17]. If the phosphor particles are flat plate, then they are expected to give a better light absorption and form a thick close solid by their orientation, resulting higher photoluminescence intensity.

Phosphor of smaller particles size can be synthesized by using liquid phase reaction methods like sol-gel [18-19], co-precipitation [20] microwave [21] and combustion [22] synthesis methods. In the liquid phase synthesis methods, each constituent (especially, activator ions) can be exactly controlled and equally dispersed throughout the phosphor materials, which is of major importance for the phosphor properties. Additional, the liquid phase synthesis methods like sol-gel, chemical combustion, and chemical co-precipitation methods are often used as low temperature paths to combine the activator ions into the phosphor host lattices. By using of surfactants and capping agents like glycerol etc. can support in the exact control of a chemical reaction and hence the morphology of the phosphor particles.

1.8 Solid-state lighting (SSL)

Light-emitting diodes (LEDs), organic light-emitting diodes (OLEDs), or light-emitting polymers are usually referred to as solid-state lighting (SSL). SSL is mostly used in a variety of lighting applications because it offers many benefits, such as:

1. Long life time — LEDs can provide 50,000 hours or more, which can minimize the maintenance costs as compared to an incandescent light bulb lasts nearly 1,000 hours.

2. Energy saving — the best commercial white LED lighting systems can provide three times the luminous efficacy (lumens/ watt) of incandescent lighting system. Colored LEDs are particularly helpful for colored lighting applications because filters are not required.

3. Better quality light output — LEDs have minimum ultraviolet and infrared radiation.

4. Intrinsically safe — LED systems are low voltage and normally cool to the touch.

5. Smaller, flexible light stuff.

6. Durable — LEDs have no filament to break, long –lasting and can withstand vibrations.

1.9 Motivation for the present study

The ultimate performances of WLED devices generally depend on the phosphors. Primarily, the excitation wavelength of the phosphor should lie in the near-UV or blue light region and thus, high wavelength conversion efficiency can be achieved by LED chips. Up to now, in contrast with blue and green phosphors, the existing red phosphors still show some limitations in terms of red color purity, efficiency and stability, which directly result in poor luminous efficiency and color rendering index (CRI) of the WLED lighting system [23-25]. Therefore the search for novel red phosphors with high efficiency, excellent chemical stability, and effective absorption in the blue or UV region is an urgent task.

Recently, Eu^{3+} activated tungstate and molybdate based phosphors for LED applications have attracted much interest due to the high chemical-physical stability, low synthetic temperature, and environmentally friendly characteristics [26-28]. In addition, these materials have a broad and an intense ligand to metal charge transfer (LMCT) band in the UV or near-UV region, which is expected to capture the emission from a GaN-based LED in this range [29]. For Eu^{3+} ion activated tunstate and molybdate compounds, the energy is transferred to the activator ions from the host lattice by a non-radiative mechanism and the red emission derived from the $^5D_0 \rightarrow {}^7F_2$ transition of Eu^{3+} is enhanced when the ion is placed in a non-centrosymmetric site.[30]

As is in centrosymmetric sites, Eu^{3+} ion emission is usually overcome by orange light. Improvements have focused on either partially substituting the tungsten of phosphors with heterogeneous metal ions (such as Mo^{6+} and Si^{4+} ions) [31] to alter the coordination environment of the Eu^{3+} luminescence center or doping them with sensitizer ions (Bi^{3+} and Li^+) to better

utilize near-UV or blue excitation from LED chips [27-28]. On the basis of these strategies, Cheetham *et al.,*[32-33] prepared various novel red phosphors including $NaM(WO_4)_{2-x}(MoO_4)_x$: Eu^{3+} (M= Gd, Y, Bi) by partially substituting MoO_4^{2-} and WO_4^{2-}. As a consequence, the charge transfer band of the phosphors from the UV region shifts towards longer wavelengths, making the luminescent system suitable for LED devices in which the excitation is within the near-UV or blue light range. Under excitation at about 400 nm, excellent efficiency of the red emission was obtained.

Although MoO_6 is generally used to substitute WO_6 to adjust the LMCT band of a tungstate phosphor because of the isomorphism effect [31-34], this strategy is not all the time suitable for all tungstate systems. For some tungstate compounds, introduction of Mo^{6+} will lead to collapse of the structure and, eventually, the quenching of the luminescence of the phosphor.
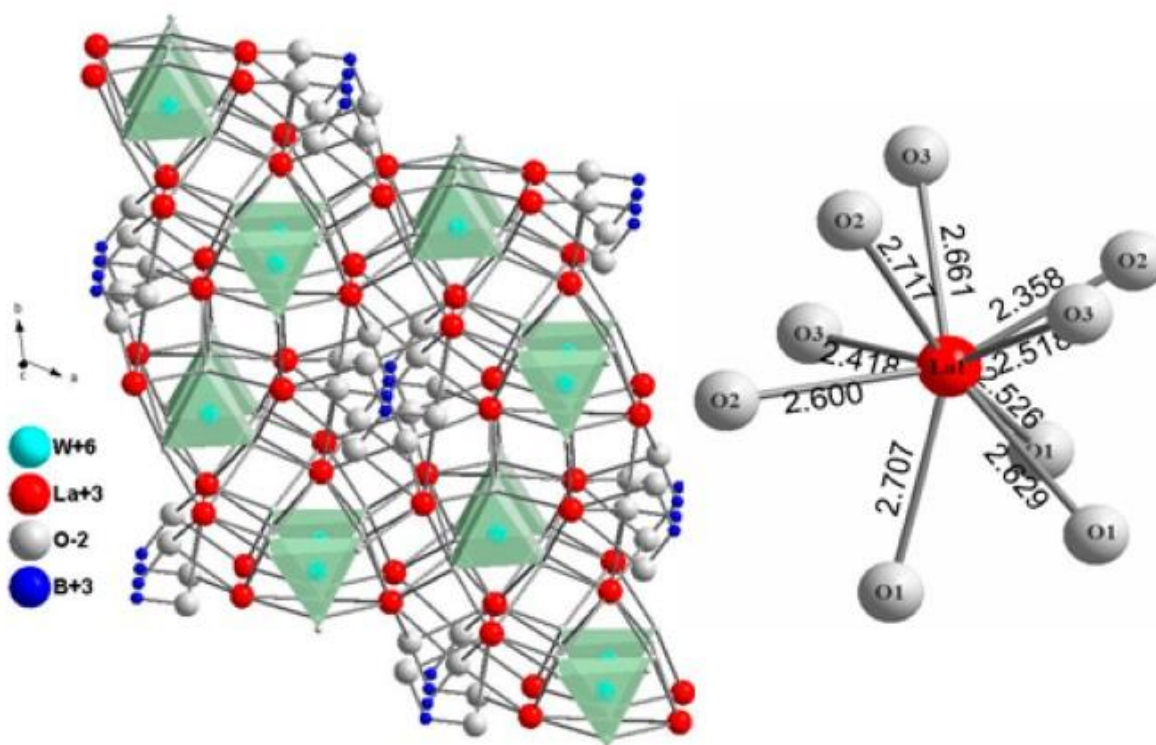

Fig 9. Crystal structure of the La_3BWO_9 host and the 9-fold coordination around La^{3+} ions [36]

Chapter 2

2. Experimental Section

2.1 Methods for Preparation of Phosphors

2.1.1 Solid State Method: In general, phosphors are synthesized majorly by solid state reaction between raw materials at high temperatures. First the high purity materials of host compounds, activator and fluxes are mixed and blended to get homogeneous mixture. Then the mixture was calcined at high temperature in a container (crucible). The fired product is then crushed, milled and then sorted to remove coarse and excessively crushed particles. In the solid state reactions high temperature firing is necessary. But, the intention of firing is not only to cause solid state reactions but also to form well crystallized particles with a suitable normal diameter. The substance added to the raw material mixture to help crystal growth is called a flux. Fluxes are commonly alkali and alkaline earth compounds (e.g. LiF, NaCl, KI, $MgCl_2$, $BaCl_2$, $CaCl_2$) or some others like NH_4F, NH_4Cl, NH_4I, B_2O_3 etc. having low melting points. When the fluxes melt, the surface tension of the liquid helps particles coagulate. [35]

2.2 Synthesis of compounds

The samples were prepared by solid state method. Chemical having high purity (99.9%) La_2O_3, MoO_3, WO_3, Eu_2O_3, Gd_2O_3, H_3BO_3 were used as precursors. All were from Sigma Aldrich. Composite mixture containing stoichiometric amounts of chemicals was taken and ground into powder, transfers the mixture into alumina crucible. **Condition 1(C1):** Fired at 650°C for 6 hours, cool it to room temperature, again ground and calcined at 1100°C for 12 hours. **Condition 2(C2)**: Fired at 650°C for 6 hours, cool it to room temperature, again ground and calcined at 1100°C for 12 hours for two times.

2.3 Characterization of Phosphors

The synthesized phosphors are characterized by using X-ray diffraction technique, SEM, DRS spectroscopy and Fluorescence spectroscopy. The powder X-ray diffraction pattern of La_2GdBWO_9 and $La_2Gd_{0.9}Eu_{0.1}BW_{1-x}Mo_xO_9$ (x = 0 − 0.4), compositions were obtained from a RIGAKU JAPAN/ULTIMA-IV Diffract meter using Ni-filtered Cu Kα radiation. The XRD measurements were carried out in the 2θ range of 10-70° with a scan speed 2 degrees per minutes. The Surface morphology, size, and shape of the materials were obtained from Scanning

Electron Microscope (SEM) (JEOL: JSM-6480 LV Scanning electron microscopy). The Diffuse reflectance Spectra (DRS) La_2GdBWO_9 and $La_2Gd_{0.9}Eu_{0.1}BW_{1-x}Mo_xO_9$ (x = 0 − 0.4), were recorded using Shimadzu Spectrophotometer (UV-2250) in the range of 200-800 nm and the barium sulphate ($BaSO_4$) used as an internal reference. The photoluminescence excitation and emission spectra of La_2GdBWO_9 and $La_2Gd_{0.9}Eu_{0.1}BW_{1-x}Mo_xO_9$ (x = 0 − 0.4), were recorded using Horiba Jobin Yvon, USA/Fluoromax 4P.

Chapter 3

3. Result and Discussion

3.1 Powder X- ray diffraction

Fig3.1a and Fig3.1b shows XRD pattern of first compounds in which a proper phase is formed by comparing it with JCPDS PDF no. 11-1070 for the standard La_3BGdWO_9 and JCPDS of MoO_3 and Gd_2O_3 for reference *(but has one impurity at 27.8 degree). This impurity may correspond to MoO_3/WO_3.). The unit cell parameters of the synthesized phosphor material are a=b=8.869(2) Å, c= 5.447(2)Å and the interfacial angles α=β=90˚, γ=120˚, the volume of the cell is 428.45Å^3 with hexagonal structure having $P6_3$ space group.
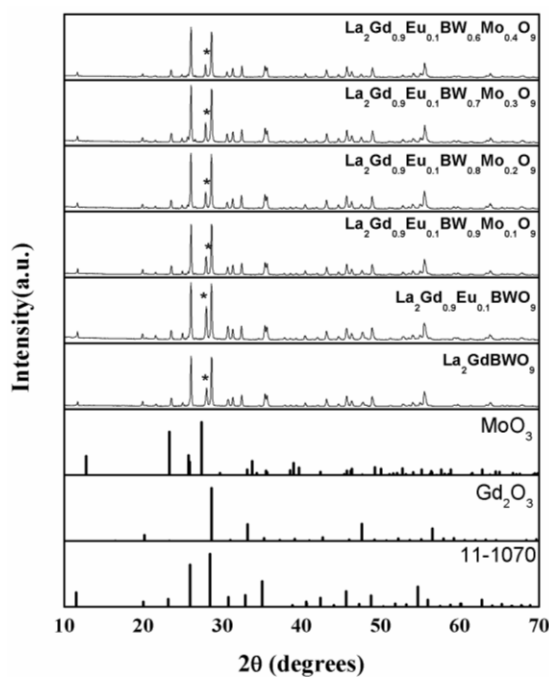
Fig 3.1a XRD pattern of C1 (*impurity MoO_3/WO_3)   **Fig.3.1b** XRD pattern of C2 (* impurity MoO3/WO3)
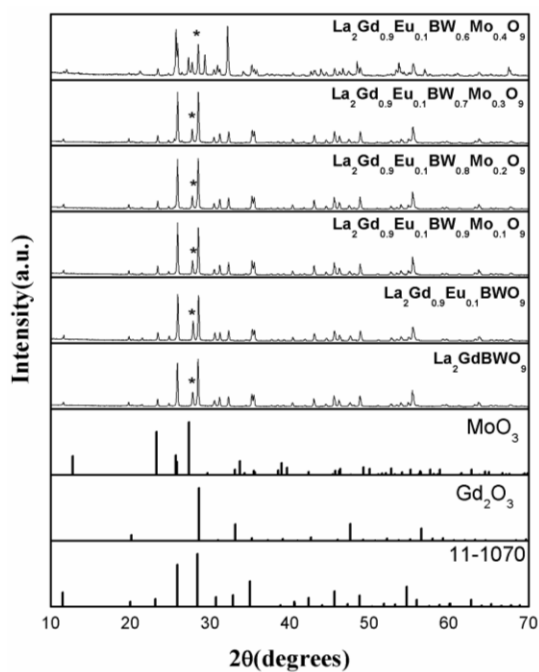
Note: After second heating see fig3.1b, more peaks are added to the composition $La_2Gd_{0.9}Eu_{0.1}BW_{0.6}Mo_{0.4}O_9$.

3.2 Scanning Electron Microscope (SEM)

Fig 3.2a and Fig 3.2b gives the morphology of the host (La_2GdBWO_9) and doped ($La_2Gd_{0.9}Eu_{0.1}BW_{0.6}Mo_{0.4}O_9$) sample. The structure is not uniform as seen in the picture which was taken after irradiating it with electron beam of 20kV and scale at 10µm and 5µm respectively.
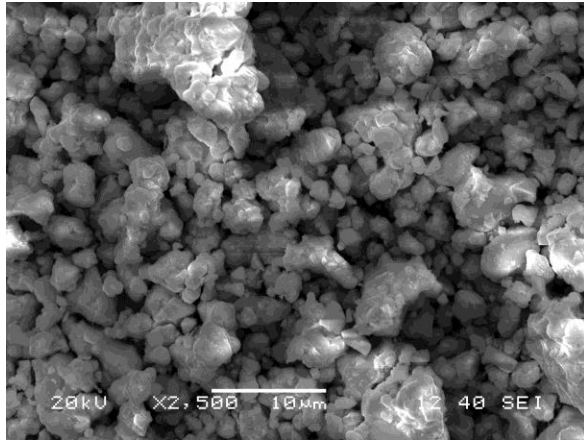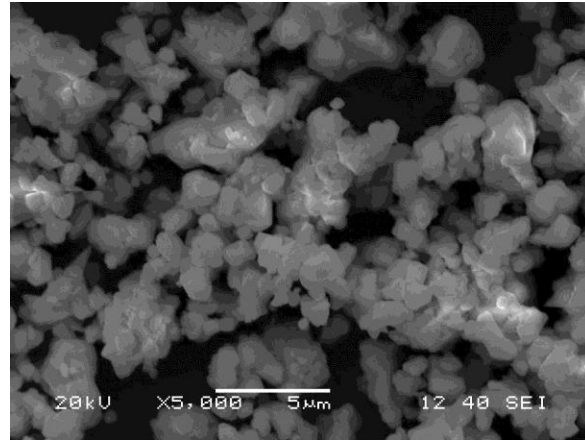

Fig 3.2a SEM image of La_2GdBWO_9 **Fig 3.2b** SEM image of $La_2Gd_{0.9}Eu_{0.1}BW_{0.6}Mo_{0.4}O_9$

3.3 Diffuse Reflectance Spectroscopy (DRS):

Fig 3.3a shows the absorption spectra of all compounds synthesized on condition1. Fig 3.3b shows the absorption of all compounds synthesized on condition2. It shows that all the compounds are absorbing in the UV region (200 to 400 nm) and Fig3.3c and Fig3.3d shows reflectance of compounds by condition1 and 2 respectively. There is a strong absorption in the visible region i.e. from 200 to 370 nm due to the host. Sharp breakdown from 370 to 400 nm, which is due to the activator Eu^{3+} (f-f transition). Broad absorption band is observed for all compositions and this band is due to charge transfer transition from O $\rightarrow$ W. In other words electronic transition from valence band (primarily oxygen 2p non-bonding character) to conduction band (arises from p* interaction between the tungsten metal ion t_{2g} orbital and oxygen). From the DRS reflectance spectra the bad gap of $La_2Gd_{0.9}Eu_{0.1}BWO_9$ is found to be 3.3498 eV shown in the fig 3.3e and remaining all band gap values are shown in Table-1, these values are calculated by using Kubelka Munk formula i.e. $(\alpha h\nu)^{1/2} \propto (h\nu - E_{gap})$ where α is absorption coefficient, h is planck's constat. The value matches with the reported value given by H.W. Eng, P.W. Barnes *et al.*,
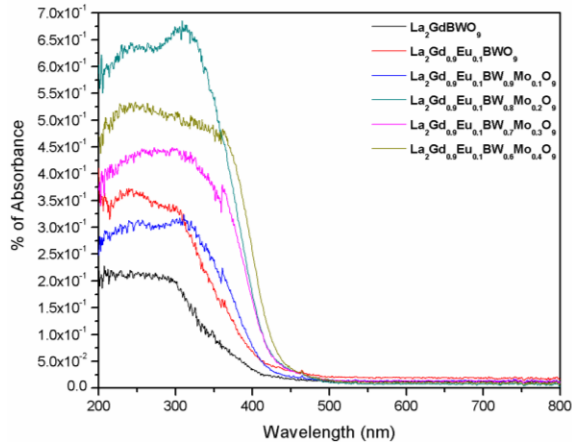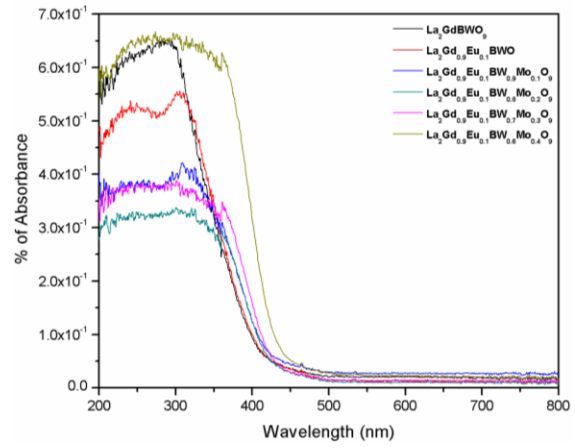
Fig 3.3a Absorption spectra of C1
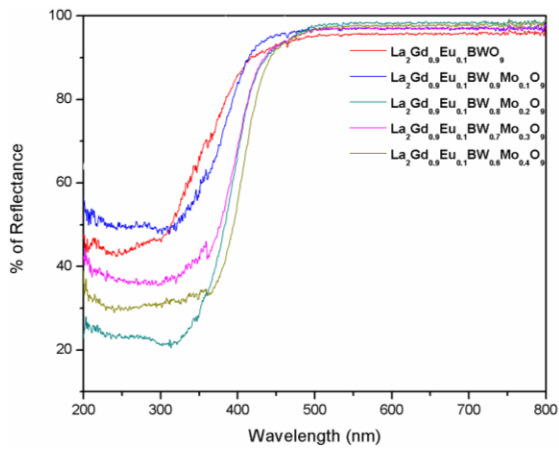

Fig3.3b Absorption spectra of C2

Fig 3.3c Reflectance spectra of C1

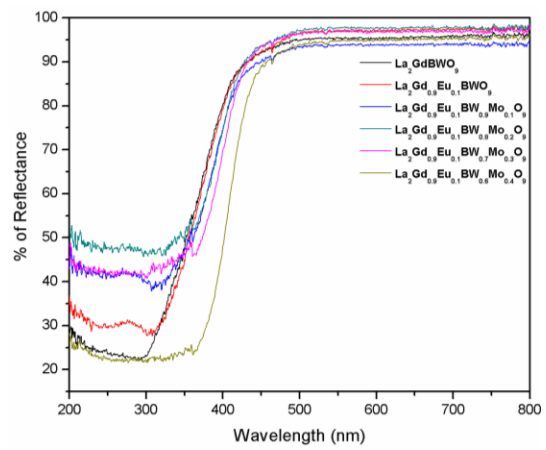**Fig3.3d** Reflectance spectra of C2
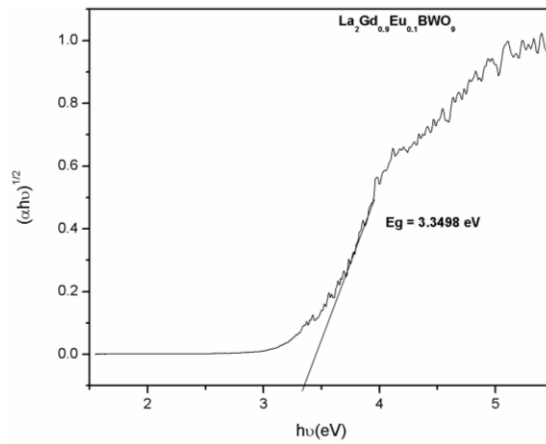
Fig 3.3e Band gap of $La_2Gd_{0.9}Eu_{0.1}BWO_9$

15

Table1. Band Gap values of synthesized compounds.

C1	
La_2GdBWO_9	3.2443
$La_2Gd_{0.9}Eu_{0.1}BWO_9$	3.3498
$La_2Gd_{0.9}Eu_{0.1}BW_{0.9}Mo_{0.1}O_9$	2.9404
$La_2Gd_{0.9}Eu_{0.1}BW_{0.8}Mo_{0.2}O_9$	2.9084
$La_2Gd_{0.9}Eu_{0.1}BW_{0.7}Mo_{0.3}O_9$	2.8711
$La_2Gd_{0.9}Eu_{0.1}BW_{0.6}Mo_{0.4}O_9$	2.8791
C2	
La_2GdBWO_9	3.2763
$La_2Gd_{0.9}Eu_{0.1}BWO_9$	3.1190
$La_2Gd_{0.9}Eu_{0.1}BW_{0.9}Mo_{0.1}O_9$	2.9324
$La_2Gd_{0.9}Eu_{0.1}BW_{0.8}Mo_{0.2}O_9$	2.7219
$La_2Gd_{0.9}Eu_{0.1}BW_{0.7}Mo_{0.3}O_9$	2.8258
$La_2Gd_{0.9}Eu_{0.1}BW_{0.6}Mo_{0.4}O_9$	2.8844

3.4 Photoluminescence Spectroscopy (PL)

The excitation spectrum of synthesized phosphor material is shown in fig 3.4a and fig3.4b. A broad absorption band is observed and this is due to charge transfer (CT) transition of oxygen to tungsten in WO_6. Sharp peaks are observed which are due to f-f electronic transition of Eu^{3+} ion. The intensity of CT band and that of f-f transition in the excitation spectrum depends on the emission wavelength monitored at 615nm.

The emission spectrum of phosphor material is shown in 3D in the fig3.4c, fig3.4d and 2D in fig3.4e and 3.4f respectively. One dominant peak at 615 nm is attributed to the f-f transition of Eu^{3+} namely $^5D_0 \rightarrow {}^7F_2$ electric dipole transition indicating that Eu^{3+} locate at the sites of non-inversion symmetry. The other emission peaks are relatively weak with respect to electric dipole transitions. La is coordinated distortedly with 9 oxygen atoms see figure 9, when Eu^{3+} is doped with the La site in the lattice, it is expected to replace the La position at the coordination site because of this distorted symmetry electron dipole mixing can take place due to this, dominant red emission at 615nm was observed in the emission spectrum.
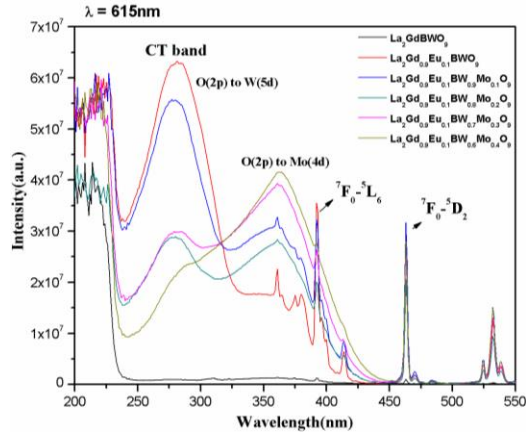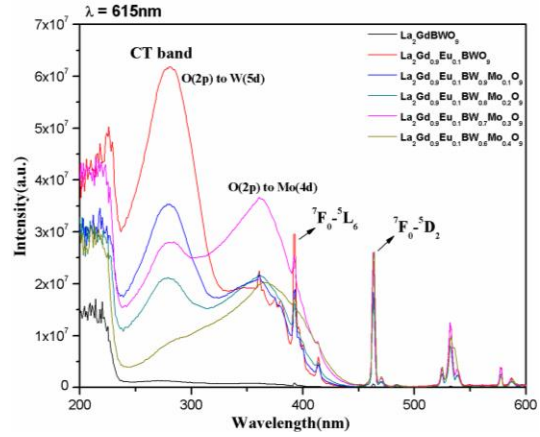
Fig3.4a Excitation spectra of C1
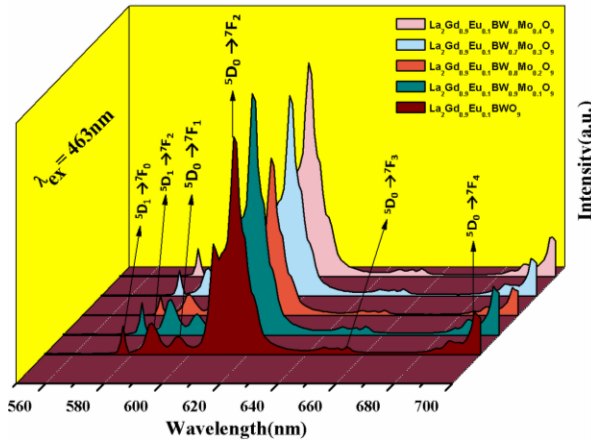

Fig 3.4b Excitation spectra of C2

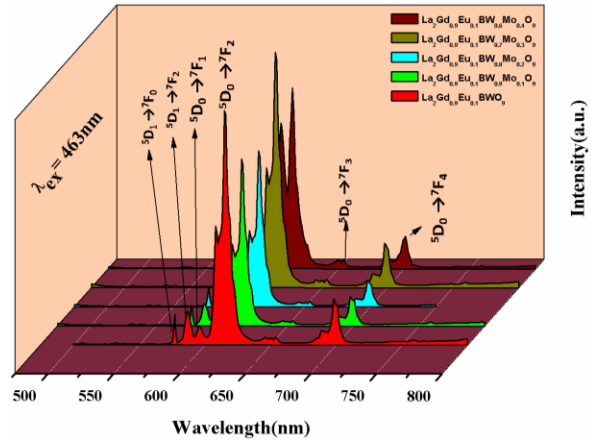**Fig 3.4c** Emission of C1
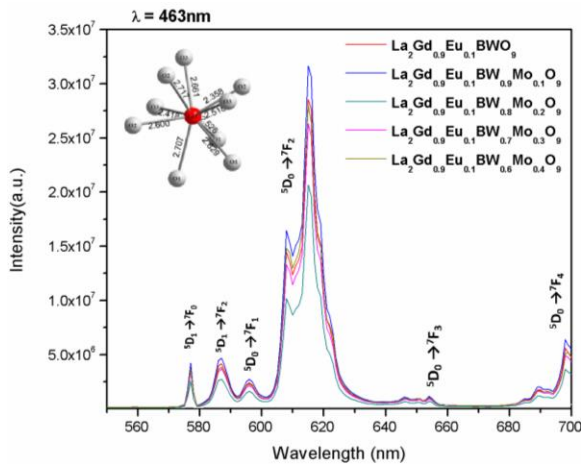

Fig 3.4d Emission of C2

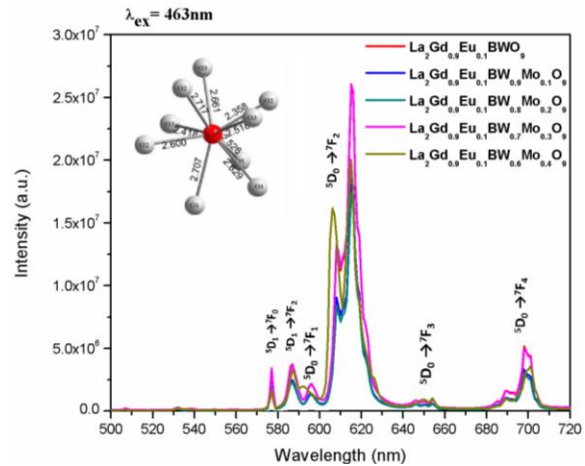**Fig3.4e** Emission spectra of condition1 (at 463nm)

Fig3.4f Emission spectra of condition2 (at 463nm)

If the structure is having centrosymmetric site than the orange emission will dominant in the spectrum ($^5D_0$ - $^7F_1$). The schematic representation of Eu^{3+} energy level is shown in Fig. 3.5g.

3.5 Commission International del'Eclairage (CIE) chromaticity coordinates

The CIE (Commission International del'Eclairage - 1931) chromaticity coordinate values of emissions for the doped compounds are calculated and is indicated by a Fig3.5a, the inset shows the photographs of doped samples taken under UV light (excited at 365 nm). The CIE values for the various concentrations are summarized in the Table-2. The intense emission from the activator Eu^{3+} ions results in red colour with the CIE chromaticity coordinate values x = 0.6647 and y = 0.3349, which were close to the National Television Standard Committee (NTSC) standard values with (x = 0.670 and y = 0.330). Hence, this red phosphor can find potential applications in the white LED based on yellow + red phosphor.
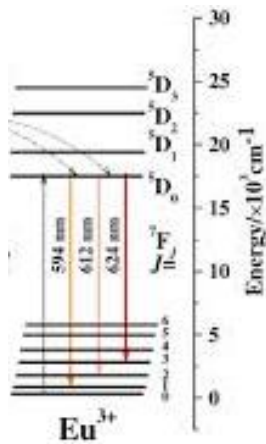

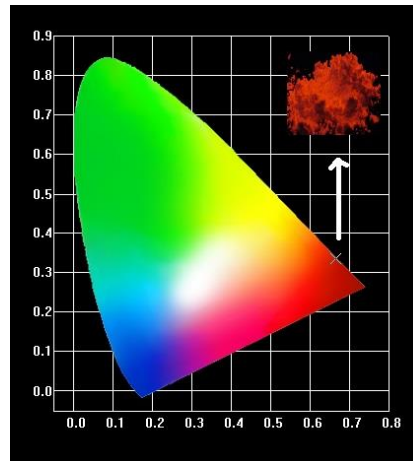
Fig3.5g. The schematic energy levels of Eu^{3+}

Fig3.5a CIE of $La_2Gd_{0.9}Eu_{0.1}BW_{0.6}Mo_{0.4}O_9$ at 463nm

Table-2 CIE values of synthesized compounds.

Condition1		
Composition	X	Y
$La_2Gd_{0.9}Eu_{0.1}BWO_9$	0.6640	0.3357
$La_2Gd_{0.9}Eu_{0.1}BW_{0.9}Mo_{0.1}O_9$	0.6639	0.3357
$La_2Gd_{0.9}Eu_{0.1}BW_{0.8}Mo_{0.2}O_9$	0.6645	0.3351
$La_2Gd_{0.9}Eu_{0.1}BW_{0.7}Mo_{0.3}O_9$	0.6644	0.3352
$La_2Gd_{0.9}Eu_{0.1}BW_{0.6}Mo_{0.4}O_9$	0.6647	0.3349
Condition2		
$La_2Gd_{0.9}Eu_{0.1}BWO_9$	0.6530	0.3465
$La_2Gd_{0.9}Eu_{0.1}BW_{0.9}Mo_{0.1}O_9$	0.6502	0.3488
$La_2Gd_{0.9}Eu_{0.1}BW_{0.8}Mo_{0.2}O_9$	0.6498	0.3479
$La_2Gd_{0.9}Eu_{0.1}BW_{0.7}Mo_{0.3}O_9$	0.6496	0.3493
$La_2Gd_{0.9}Eu_{0.1}BW_{0.6}Mo_{0.4}O_9$	0.6501	0.3492

3.6 UV images at wavelength 365nm

Host compound i.e. La_2GdBWO_9 under UV 365nm shows no color as shown in Fig 3.6a but Eu-doped compound shows intense red color under UV 365nm as shown in Fig 3.6b which indicates the presence of Eu in the host lattice.
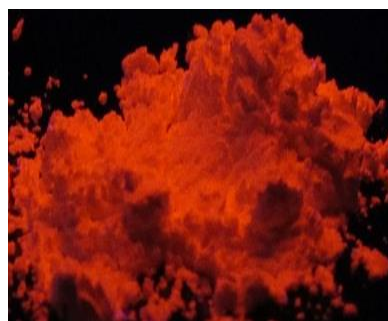

Fig 3.6a Host compound under UV 365nm

Fig 3.6b Doped compound under UV 365nm

Chapter 4

4.1 Summary and Conclusion

The compounds La_2GdBWO_9 and $La_2Gd_{0.9}Eu_{0.1}BW_{1-x}Mo_xO_9$ (x = 0 – 0.4), have been synthesized by solid state method. The compositions have been characterized by X-ray diffraction, photoluminescence spectroscopy, diffused reflectance spectroscopy, scanning electron microscopy and CIE coordinates. The pore size, morphology and shape of the compound have studied by SEM. The excitation spectra show a broad emission whereas the emission spectra show sharp peaks. The photoluminescence studies reveal an excellent red emission excitation which may be used as a red phosphor for the white LEDs based on blue or near UV + Yellow phosphor.

4.2 Future Work:

1. Single phase compositions to be synthesized.

2. Synthesized phosphor to be examined for LED fabrication by combination with yellow phosphors.

3. The work to be extended for the other rare earth ions as an activator like Sm^{3+}, Tb^{3+} etc.

References:

1. Blasse G, Grabmaier B.C, Luminescent Materials, Springer-Verlag, 1994

2. D.F. Shriver, P.W. Atkins and C.K. Langford (1990) Inorganic chemistry, Oxford University Press (Chapter 14 and 18).

3. Blasse G (1992) Int. Revs Phys. Chem. 11:71

4. Henderson B, Imbusch GF (1989) Optical spectroscopy of inorganic solids. Clarendon, Oxford

5. Judd BR (1962) Phys. Rev. 127:750; Ofelt GS (1962) J. Chem. Phys. 37:511

6. Peacock RD (1975) Structure and Bonding 22:83

7. Blassé G (1976) Structure and Bonding 26:43

8. Blasse G (1992) Int Rev Phys Chem 11:71

9. Blasse G, Schipper W, Hamelink JJ (1991) Inorg Chim Acta 189:77

10. Williams F, Berry DE, Bernard JE, p 409 in Dibartolo B (ed) (1980) Radiationless processes. Plenum, New York

11. J. Holsa, H. Jungner, M. Lastusaari, J. Niittykoski, *J. Alloys Compd*. **326** (2001) 323.

12. W.Y. Jia, H.B. Yuan, L.Z. Lu, H.M. Liu, W.M. Yen, *J. Cryst. Growth*, **200** (1999) 179.

13. M. Peng, Z.W. Pei, G.G. Hong, *Chem. Phys. Lett*. **371** (2003) 1.

14. Y.H. Lin, Z.T. Zhang, F. Zhang, Z.L. Tang, Q.M. Chen, *Mater.Chem.Phys*.**65** (2000)103.

15.. A. Nag, T.R.N. Kutty, *J. Alloys Compd*. **354** (2003) 221.

16. V. Shankar, H. Chander, H. Divi, P.K. Ghosh, US Patent 0183807 A1.

17. D. Jia, *Opt. Mater*. **22** (2003)65.

18. T. Peng, L. Huajun, H. Yang, C. Yan, *Mater. Chem. Phys*.**85** (2004) 68.

19. C.H. Lu, W.T. Hsu, C.H. Huang, S.V. Godbole, B.M. Cheng, *Mater.Chem. Phys*. **90**(2005) 62.

20. Y. Pan, M. Wu, Q. Su, *Mater. Sci. Eng* .B**106** (2004) 251.

21. Y.Chen, J. Wang, M. Gong, Q. Su, *J. Solid State Chem*. **180** (2007) 1165.

22. Z. Chen, Y. Yan, J. Liu, Y. Yin, H. Wen, J. Zao, D. Liu, H. Tian, C. Zhang, S. Li, *J.Alloys Compd*. **473** (2009) L13.

23 Jia, L.; Shao, Z.; Lu, Q.; Tian, Y.; Han, J. Ceram. Int. 2014, 40, 793-743.

24 Zhang, X.; Zhang, J.; Gong, M. Opt. mater. 2014, 36, 850-853.

25 Axe, J. D.; Weller, P. F. J. Chem Phys. 1964, 40, 3066-3069.

26 Guo, Y.; Sun, M.; Guo, W.; Ren, F.; Chen, D. Opt. Laser Technol. 2010, 42, 1328-1331.

27 Jin, H.; Wu, H.; Tian, L. J. Lumin. 2012, 132, 1188-1191.

28 Tian, L.; Yang, P.; Wu, H.; Li, F. J. Lumin. 2010, 130, 717-721.

29 Dutta, P. S.; Khanna, A. ECS J. Solid State Sci. Technol. 2012, 2, R3153-3167.

30 Huang, J.; Luo, H.; Zhou, P.; Yu, X.; Li, Y. J. Lumin. 2007, 126, 881-885.

31 Li, H.; Yang, H. K.; Moon, B. K.; Choi, B. C.; Jeong, J. H.; Jang, K.; Lee, H. S.; Yi, S. S. Inorg. Chem. 2011, 50, 12522-12530.

32 Neeraj, S.; Kijima, N.; Cheetham, A. K. Chem. Phys. Lett. 2004, 387, 2-6.

33 Neeraj, S.; Kijima, N.; Cheetham, A. K. Solid State commun. 2004, 131, 65-69.

34 Li, H.; Yang, H. K.; Moon, B. K.; Choi, B. C.; Jeong, J. H.; Jang, K.; Lee, H. S.; Yi, S. S. J. Alloys Compd. 2011, 509, 8788-8793.

35. G.F.J. Garlick, Luminescent Materials, Oxford University Press, UK, 1949

36. Jinping Huang,* Binghu Hou, Hongya Ling, Jie Liu, and Xibin Yu, Inorg. Chem. 2014, 53, 9541−9547

37. Zhiguo Xia *et al.,* 2012 *J. Phys. D: Appl. Phys.* **45** 015302. doi:10.1088/0022-3727/45/1/015302